

DOI: 10.1002/cbic.201300567

Unlocked Nucleic Acids with a Pyrene-Modified Uracil: Synthesis, Hybridization Studies, Fluorescent Properties and i-Motif Stability

Pavla Perlíková,^[a, b] Kasper K. Karlsen,^[a] Erik B. Pedersen,^[a] and Jesper Wengel^{*[a]}

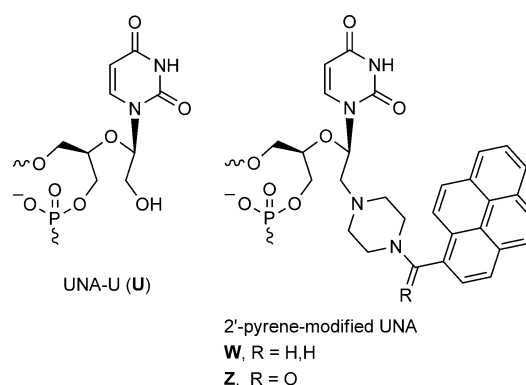
The synthesis of two new phosphoramidite building blocks for the incorporation of 5-(pyren-1-yl)uracilyl unlocked nucleic acid (UNA) monomers into oligonucleotides has been developed. Monomers containing a pyrene-modified nucleobase component were found to destabilize an i-motif structure at pH 5.2, both under molecular crowding and noncrowding conditions. The presence of the pyrene-modified UNA monomers in DNA strands led to decreases in the thermal stabilities of DNA*/DNA and DNA*/RNA duplexes, but these duplexes' thermal stabilities were better than those of duplexes containing unmodified UNA monomers. Pyrene-modified UNA monomers incorporat-

ed in bulges were able to stabilize DNA*/DNA duplexes due to intercalation of the pyrene moiety into the duplexes. Steady-state fluorescence emission studies of oligonucleotides containing pyrene-modified UNA monomers revealed decreases in fluorescence intensities upon hybridization to DNA or RNA. Efficient quenching of fluorescence of pyrene-modified UNA monomers was observed after formation of i-motif structures at pH 5.2. The stabilizing/destabilizing effect of pyrene-modified nucleic acids might be useful for designing antisense oligonucleotides and hybridization probes.

Introduction

Nucleic acids play key roles in numerous cellular processes in which they adopt various structures and perform various functions. Chemical modifications can endow naturally occurring nucleic acids with unique properties, and chemically modified nucleic acids have therefore been widely explored for molecular diagnostics and therapeutic applications.

Unlocked nucleic acids (UNAs, 2',3'-seco-RNAs) are acyclic analogues of RNA that lack C–C bonds between 2'- and 3'-carbon atoms (Scheme 1).^[1] Opening of the furanose ring leads to increased flexibility in an UNA monomer. This has a negative effect on the stabilities of nucleic acid duplexes,^[2–6] but can improve mismatch discrimination.^[3,6] UNA monomers were also found to modulate the stabilities of i-motif^[7] and G-quadruplex^[8] structures. UNA monomers therefore meet the requirements for applications in antisense oligonucleotides,^[9,10] siRNA constructs^[11] and aptamer development.^[12] Chemical synthesis of UNA phosphoramidite building blocks is simple,^[2,3] and an UNA monomer can be incorporated into oligonucleotides either through the O3^[2,3] or the O2^[2,4,9] atom. The sugar moiety of an UNA monomer can easily be conjugated with, for



Scheme 1. UNA monomers.

example, ligands for complexation of metal ions^[13] or attachment of fluorescent labels^[6] such as pyrene.

Pyrene units are widely used for oligonucleotide functionalization, due to pyrene's fluorescent properties and its aromatic stacking and duplex intercalating abilities.^[14,15] A pyrene moiety can be attached either to the sugar part of the nucleotide or to the nucleobase. It can also substitute the nucleobase or be used in non-nucleosidic monomers such as intercalating nucleic acid (INA)^[16] or twisted intercalating nucleic acid (TINA) monomers.^[17]

2'-Pyrene-modified UNA oligonucleotides (incorporating monomers W or Z, Scheme 1) display increased fluorescence upon hybridization to DNA, together with pyrene excimer emission, and have been employed in development of molecular beacons.^[18] Furthermore, introduction of the pyrene moiety

[a] Dr. P. Perlíková, Dr. K. K. Karlsen, Prof. E. B. Pedersen, Prof. J. Wengel
Nucleic Acid Center, Department of Physics, Chemistry, and Pharmacy
University of Southern Denmark
Campusvej 55, 5230 Odense M (Denmark)
E-mail: jwe@sdu.dk

[b] Dr. P. Perlíková
Institute of Organic Chemistry and Biochemistry
Academy of Sciences of the Czech Republic
Flemingovo nám. 2, 16610 Prague 6 (Czech Republic)

Supporting information for this article is available on the WWW under
<http://dx.doi.org/10.1002/cbic.201300567>.

into UNA monomers led to stabilization of nucleic acid duplexes relative to unmodified UNA, whereas the strong mismatch discrimination capabilities of appropriately designed UNA oligomers were maintained.^[6] The pyrene units of 2'-pyrene-modified UNA monomers were found to be located in the major groove in the nucleic acid duplex.^[6]

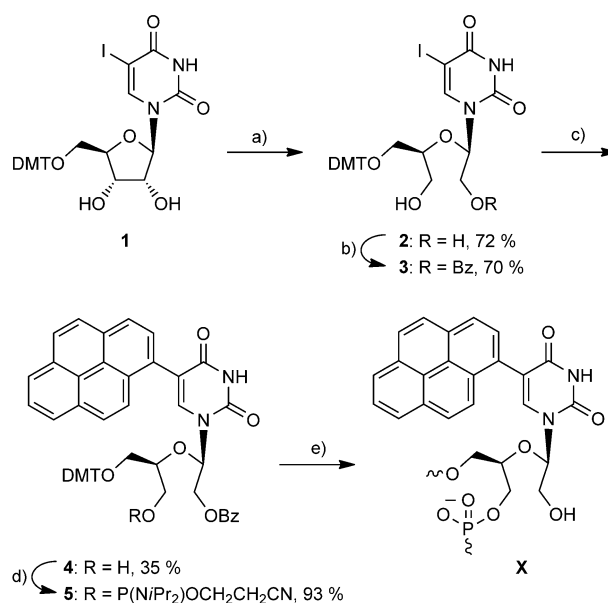
The positioning of a functionality into the major groove of a nucleic acid duplex can conveniently be achieved by functionalization of the 5-position of a pyrimidine nucleobase. Direct conjugation of the pyrene with this nucleobase component is expedient because covalent linking between the pyrene moiety and a pyrimidine base leads to strong electron coupling between the two aromatic units, resulting in interesting fluorescence properties such as charge transfer emission.^[19,20] Oligonucleotides incorporating 5-(pyren-1-yl)-2'-deoxyuridine units have therefore been intensively used for studies of electron-transfer processes in DNA.^[21-23] Furthermore, oligonucleotides containing 2'-deoxyuridine monomers with a fluorescent label in the 5-position were found to change fluorescence properties upon formation of an i-motif structure, thus allowing probing of i-motifs.^[24]

Preparation of oligonucleotides (ONs) containing UNA monomers bearing pyrene substituents at position 5 of the uracil base is of interest because these monomers combine the flexibility of the UNA with the stabilization effect of the pyrene moiety in the major groove of a nucleic acid duplex. Furthermore, 5-(pyren-1-yl)uracilyl nucleotides show interesting fluorescence properties.^[19-23] In this report we describe the synthesis of two new phosphoramidite building blocks for the incorporation of 5-(pyren-1-yl)uracilyl UNA monomers **X** and **Y** (Schemes 2 and 3) into ONs. We have studied the thermal stabilities and the steady-state fluorescence emission and UV/visible spectra of DNA*/DNA and DNA*/RNA duplexes of oligonucleotides containing 5-pyrene-modified UNA monomers, as well as those of DNA*/DNA and DNA*/RNA duplexes with bulge-incorporated 5-pyrene-modified UNA monomers. The thermal stabilities and the fluorescence and UV/visible absorption properties of i-motif-forming ONs with 5-pyrene-modified UNA monomers are also reported.

Results and Discussion

Synthesis

A synthetic approach to the phosphoramidite building blocks **5** and **8** from DMT-protected 5-iodouridine **1**^[25] was developed. 2',3'-Bond cleavage was accomplished by treatment with NaIO_4 , and subsequent reduction of the dialdehyde intermediate with NaBH_4 afforded the acyclic derivative **2** in 72% yield (Scheme 2). Selective benzylation with benzoyl chloride in the presence of DBU in CH_2Cl_2 at -78°C provided O2'-benzoate **3** in 70% yield. Formation of a by-product tentatively assigned as the corresponding O3'-benzoate was observed, but the compound was not isolated. A pyrene moiety was introduced into the 5-position in benzoate **3** by means of a Suzuki-Miyaura cross-coupling reaction with pyrene-1-boronic acid under palladium catalysis. The conditions used by Wagen-



Scheme 2. a) i: $\text{NaIO}_4/1,4\text{-dioxane, H}_2\text{O, RT}$; ii: $\text{NaBH}_4/1,4\text{-dioxane, H}_2\text{O, RT}$; b) BzCl (Bz = benzoyl), $\text{DBU}/\text{CH}_2\text{Cl}_2, -78^\circ\text{C}$; c) pyrene-1- $\text{B}(\text{OH})_2, \text{Na}_2\text{CO}_3, \text{PPh}_3, \text{Pd}(\text{OAc})_2/\text{toluene}/\text{H}_2\text{O}, 100^\circ\text{C}$; d) $\text{P}(\text{Cl})(\text{NiPr}_2)\text{OCH}_2\text{CH}_2\text{CN}, \text{DIPEA}/\text{CH}_2\text{Cl}_2, \text{RT}$; e) oligonucleotide synthesis.

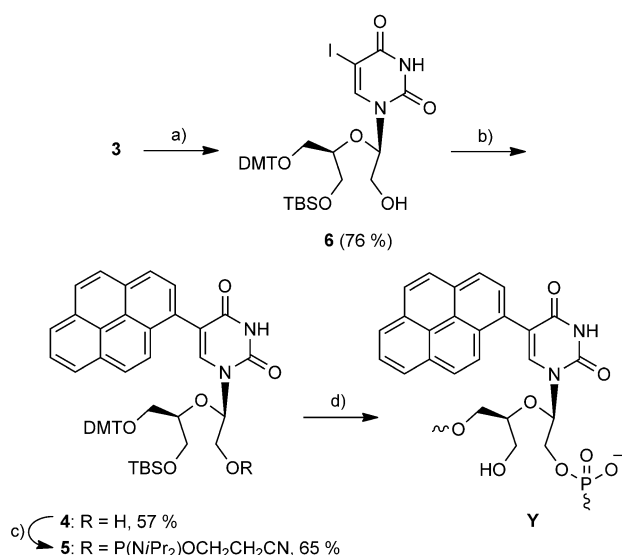
knecht^[20,23] could not be applied because of rapid hydrolysis of the benzoyl group in the presence of NaOH , so milder conditions with Na_2CO_3 as a base were used.^[26] Even though an excess (3 equiv) of the boronic acid was used, partial deiodination of the starting material was observed, but the pyrenyl-substituted nucleoside **4** was obtained in 35% yield. Subsequent O3'-phosphitylation of nucleoside **4** by treatment with 2-cyanoethyl-*N,N*-diisopropylchlorophosphoramidite afforded phosphoramidite **5** in 93% yield.

The synthesis of phosphoramidite **8** (Scheme 3) started with silylation of the 3'-hydroxy group of nucleoside **3** by treatment with TBSCl in pyridine, followed by removal of the 2'-*O*-benzoyl group by hydrolysis with NaOH , leading to O3'-silylated nucleoside **6** in 76% yield over the two steps. Subsequent Suzuki-Miyaura cross-coupling with pyrene-1-boronic acid in the presence of $\text{Na}_2\text{CO}_3, \text{PPh}_3$ and $\text{Pd}(\text{OAc})_2$ in toluene/water at 100°C afforded nucleoside **7** in 57% yield. Finally, O2'-phosphitylation of nucleoside **7** provided phosphoramidite **8** in 65% yield.

The phosphoramidite building blocks **5** and **8** were used in an automated DNA synthesizer to incorporate 3'-linked monomer **X** and 2'-linked monomer **Y**, respectively, into ONs [**ON1-6** (Table 1) and **ON7** and **ON8** (Table 5, below)].

Thermal denaturation studies

The thermal stabilities (T_m values) of duplexes formed between ONs with single or double incorporation of monomer **X** or **Y** (DNA*) and complementary DNA or RNA were studied (Table 1). The T_m values of DNA*/DNA and DNA*/RNA duplexes with single incorporation of either **X** or **Y** in position 10 (**ON1**, **ON4**) were determined to be approximately 4°C lower than



Scheme 3. a) i: TBSCl/py, RT; ii: NaOH/MeOH, RT; b) pyrene-1-B(OH)₂, Na₂CO₃, PPh₃, Pd(OAc)₂/toluene/H₂O, 100 °C; c) P(Cl)(NiPr₂)OCH₂CH₂CN, DIPEA/CH₂Cl₂, RT; d) oligonucleotide synthesis.

the T_m values of the corresponding unmodified references, showing the destabilization effect of the pyrene-modified UNA monomers. In addition, the thermal stabilities of DNA*/DNA and DNA*/RNA duplexes with two incorporations of **X** or **Y** were lower than those of the unmodified duplexes. The duplexes in which the two insertions were separated by a single nucleotide were less stable than those in which the two insertions were nine bases apart. The T_m values of duplexes containing UNA monomers **X** and **Y** were similar to each other and therefore not dependent on the way in which the pyrene-modified UNA monomer was incorporated into the oligonucleotide backbone. Generally, the DNA*/DNA duplexes were more stable than the DNA*/RNA duplexes; this indicates that the pyrene moiety fits better into the major groove of a DNA/DNA duplex (see also UV/visible absorption studies). Even though duplexes containing pyrene-modified UNA monomers were found to be less stable than the unmodified references,

the presence of the pyrene moiety in the 5-position led to increases of 2–11 °C in their thermal stabilities relative to their counterparts containing unmodified UNA monomer (**U**).^[6] The stabilities of duplexes of ONs containing monomers **X** and **Y** were found to be similar to those of duplexes containing 2'-pyrene-modified UNA monomers **W** and **Z** (Scheme 1).^[6] It follows that major groove interactions of the pyrene moiety improve the duplex thermal stability regardless of whether the pyrene is attached through the 5- or the 2'-position of an UNA monomer.

Mismatches were introduced into position 11 (juxtaposition to monomers **X** and **Y** in **ON1** and **ON4**) in the nucleic acid duplexes. T_m values were determined, and ΔT_m values relative to fully matched duplexes of the studied ONs were calculated (Table 1). Singly modified ONs (**ON1**, **ON4**) showed mismatch discrimination similar to or slightly lower than that of the unmodified duplexes. Only in the case of the DNA*/RNA duplex of **ON4**—with a G:U mismatch—was the discrimination higher than for the unmodified duplex. Mismatch discrimination capabilities of modified ONs containing two incorporations of **X** or **Y** separated by one base (**ON2**, **ON5**) were low, and the ΔT_m values ranged from –3 to +1 °C. On the other hand, when incorporations of **X** and **Y** were nine bases apart (**ON3**, **ON6**) mismatch discrimination was improved to 9–12 °C.

Mismatches were also introduced at position 10 (position directly opposite to monomers **X** and **Y** in **ON1**) in the duplexes (Table 2). Poor mismatch discrimination was observed for ONs **ON1**, **ON2**, **ON4** and **ON5**. For these ONs the ΔT_m values ranged from –3 to +1 °C. However, the duplexes of oligonucleotides **ON3** and **ON6**, each containing two incorporations separated by nine bases, showed highly efficient mismatch discrimination (5–14 °C). The mismatch discrimination capabilities of ONs containing monomers **X** and **Y** follow the same trend as seen with other previously reported UNA monomers (**U**, **W**, **Z**).^[3,6]

The thermal stabilities of duplexes containing monomers **X** and **Y** incorporated as single-nucleotide bulges were also studied (Table 3). DNA*/DNA duplexes with single bulge-incorporated **X** or **Y** (**ON1** and **ON4**) showed T_m values similar to those of the unmodified fully matched dsDNAs, whereas the corre-

Table 1. Thermal denaturation temperatures (T_m)^[a] of matched and mismatched duplexes based on complementary DNA and RNA strands with mismatches in the central position 11 of the complementary strand.

Code	Sequence 3'-ACG TGA CAT ABA GAC ATG GTA	B (DNA)				B (RNA)			
		C	A	G	T	C	A	G	U
DNA	5'-TGC ACT GTA TGT CTG TAC CAT	63.1	[–10.1]	[–8.6]	[–7.5]	63.3	[–10.4]	[–8.2]	[–7.9]
ON1	5'-TGC ACT GTA XGT CTG TAC CAT	58.9	[–8.0]	[–7.6]	[–6.4]	57.7	[–8.1]	[–6.8]	[–5.0]
ON2	5'-TGC ACT GTA XGX CTG TAC CAT	52.0	[–2.5]	[–2.3]	[–2.3]	48.5	[0.0]	[+0.7]	[–0.4]
ON3	5'-TGC ACX GTA TGT CTG XAC CAT	55.9	[–12.3]	[–9.8]	[–8.9]	51.7	[–12.3]	[–9.0]	[–9.4]
ON4	5'-TGC ACT GTA YGT CTG TAC CAT	58.9	[–8.2]	[–8.2]	[–5.5]	58.3	[–8.5]	[–4.9]	[–8.7]
ON5	5'-TGC ACT GTA YGY CTG TAC CAT	51.7	[–2.4]	[–1.6]	[–2.0]	49.8	[–0.2]	[–0.3]	[–1.2]
ON6	5'-TGC ACY GTA TGT CTG YAC CAT	55.9	[–12.0]	[–9.8]	[–8.7]	52.2	[–12.4]	[–9.7]	[–9.6]

[a] T_m values (°C) were measured as the maxima of the first derivatives of the thermal melting curves (A_{260} vs. temperature) recorded in medium-salt buffer (100 mM NaCl, 0.1 mM EDTA, 10 mM NaH₂PO₄, 5 mM Na₂HPO₄, pH 7.0) with use of 1.0 μM concentrations of the two strands. ΔT_m values for mismatches are given in brackets. ΔT_m values were calculated relative to fully matched duplexes of studied ONs. [b] In RNA targets, uracil bases are present instead of thymine bases.

Table 2. Thermal denaturation temperatures (T_m)^[a] of matched and mismatched duplexes based on complementary DNA and RNA strands with mismatches directly opposite the modification (position 10).

Code	Sequence	B (DNA)				B (RNA)			
		A	G	T	C	A	G	U	C
DNA	5'-TGC ACT GTA TGT CTG TAC CAT	63.1	[−5.7]	[−7.8]	[−9.4]	63.3	[−4.0]	[−7.6]	[−9.0]
ON1	5'-TGC ACT GTA XGT CTG TAC CAT	58.9	[+0.6]	[−1.7]	[−2.6]	57.7	[+0.8]	[−0.8]	[−2.2]
ON2	5'-TGC ACT GTA XGX CTG TAC CAT	52.0	[−0.4]	[−2.1]	[−1.0]	48.5	[−2.6]	[−0.6]	[−1.8]
ON3	5'-TGC ACX GTA TGT CTG XAC CAT	55.9	[−5.9]	[−9.1]	[−11.4]	51.7	[−5.5]	[−8.3]	[−12.6]
ON4	5'-TGC ACT GTA YGT CTG TAC CAT	58.9	[−0.8]	[−2.1]	[−2.0]	58.3	[−1.0]	[−1.3]	[−2.6]
ON5	5'-TGC ACT GTA YGY CTG TAC CAT	51.7	[−0.8]	[−2.6]	[−0.7]	49.8	[−2.3]	[−0.6]	[−1.9]
ON6	5'-TGC ACY GTA TGT CTG YAC CAT	55.9	[−6.6]	[−9.5]	[−12.9]	52.2	[−4.9]	[−8.7]	[−14.4]

[a], [b] See the footnotes of Table 1.

Table 3. Thermal denaturation temperatures (T_m) of matched duplexes based on complementary DNA and RNA strands and of duplexes incorporating bulges.

Code	Sequence	T_m [°C] ^[a]	
		DNA	RNA
DNA/RNA ^[b]	3'-ACG TGA CAT -CA GAC ATG GTA		
DNA	5'-TGC ACT GTA -GT CTG TAC CAT	61.7	63.3
DNA bulge	5'-TGC ACT GTA TGT CTG TAC CAT	57.4	59.2
		[−4.3]	[−4.1]
UNA1	5'-TGC ACT GTA UGT CTG TAC CAT	58.2	59.3
		[−3.5]	[−4.0]
ON1	5'-TGC ACT GTA XGT CTG TAC CAT	61.9	61.9
		[+0.2]	[−1.4]
ON4	5'-TGC ACT GTA YGT CTG TAC CAT	61.8	60.5
		[+0.1]	[−2.8]
DNA/RNA ^[b]	3'-ACG TGA CAT -C- GAC ATG GTA		
DNA	5'-TGC ACT GTA -G- CTG TAC CAT	62.2	62.1
DNA bulge	5'-TGC ACT GTA TGT CTG TAC CAT	49.4	51.7
		[−12.8]	[−10.4]
UNA2	5'-TGC ACT GTA UGU CTG TAC CAT	47.8	50.6
		[−14.4]	[−11.5]
ON2	5'-TGC ACT GTA XGX CTG TAC CAT	55.0	52.8
		[−7.2]	[−9.3]
ON5	5'-TGC ACT GTA YGY CTG TAC CAT	58.1	53.7
		[−4.1]	[−8.4]
DNA/RNA ^[b]	3'-ACG TG- CAT ACA GAC -TG GTA		
DNA	5'-TGC AC- GTA TGT CTG -AC CAT	63.6	63.4
DNA bulge	5'-TGC ACT GTA TGT CTG TAC CAT	50.2	51.8
		[−13.4]	[−11.6]
UNA3	5'-TGC ACU GTA TGT CTG UAC CAT	50.7	53.0
		[−13.6]	[−10.4]
ON3	5'-TGC ACX GTA TGT CTG XAC CAT	62.6	62.1
		[−1.0]	[−1.3]
ON6	5'-TGC ACY GTA TGT CTG YAC CAT	65.4	60.3
		[+1.8]	[−3.1]

[a] T_m values (°C) were measured as the maxima of the first derivatives of the thermal melting curves (A_{260} vs. temperature) recorded in medium-salt buffer (100 mM NaCl, 0.1 mM EDTA, 10 mM NaH_2PO_4 , 5 mM Na_2HPO_4 , pH 7.0) with 1.0 μM concentrations of the two strands. ΔT_m values for duplexes containing bulges are given in brackets. Unmodified fully matched DNA/DNA or DNA/RNA duplexes were used as references. U=uracil-1-yl UNA monomer. [b] In RNA targets, uracil bases are present instead of thymine bases.

sponding DNA*/RNA duplexes were 1–3 °C less stable than the unmodified fully matched DNA/RNA duplexes. On the other hand, the two duplexes containing single bulge-incorporated

UNA monomer **U** (**UNA1**) units were both found to be approximately 4 °C less stable than the corresponding unmodified fully matched duplexes.

Introduction of two bulge-incorporations separated by one base (**UNA2**, **ON2** and **ON5**) had a destabilizing effect on both DNA*/DNA and DNA*/RNA duplexes, with the duplex stabilities following the order $Y > X \gg U$ with respect to the introduced modifications.

Finally, thermal stabilities of nucleic acid duplexes containing two bulge-incorporations separated by nine bases (**UNA3**, **ON3** and **ON6**) were studied. The presence of two bulge-incorporated UNA monomers **U** (**UNA3**) led to significant destabilization of the duplexes. In contrast, DNA*/DNA and DNA*/RNA duplexes containing two bulge-incorporated monomers **X** (**ON3**) showed only minor thermal destabilization. The presence of two bulge-incorporated monomers **Y** separated by nine bases (**ON5**) led to stabilization of the DNA*/DNA duplex by 2 °C and to destabilization of the DNA*/RNA duplex by 3 °C relative to the fully matched unmodified duplexes. The data also showed that generally the T_m values for the duplexes containing bulge-incorporated monomers **X** and **Y** were higher for DNA*/DNA duplexes than for DNA*/RNA duplexes, thus indicating that bulge-incorporated UNA monomers with the pyrene-modified nucleobase are better able to adapt to the conformation of a DNA/DNA duplex than to that of a DNA/RNA duplex. Furthermore, bulge-containing duplexes containing pyrene-modified UNA monomers were always significantly more stable than unmodified duplexes containing DNA-T bulges. It is also important to mention that duplexes with bulge-incorporated monomers **X** and **Y** were 2–10 °C more stable than fully matched duplexes of **ON1–6** with complementary strands (Table 1).

The substantial differences between the stabilities of matched and bulge-containing duplexes might be exploitable for the development of antisense oligonucleotides and hybridization probes and for strand invasion studies. The increased stabilities of the bulge-containing duplexes are presumably due to intercalation of the pyrenyl moiety into the duplex (see also UV/visible absorption studies). A B-type duplex is less compressed and has more efficient nucleobase overlap than an A-type duplex;^[15] this is why the pyrene moiety is able to intercalate favourably into a DNA/DNA duplex, resulting in higher thermal stabilities of DNA*/DNA duplexes containing

Table 4. Thermal denaturation temperatures (T_m) of DNA duplexes containing bulges and effects of the central mismatch (position 11 in **ON6**).

Sequence (code)	T_m [°C] ^[a]
3'-ACG TG- CAT ABA GAC -TG GTA 5'-TGC AC- GTA TGT CTG -AC CAT (DNA)	B=C [A; G; T] 63.6 [-10.7; -8.7; -8.0]
5'-TGC ACT GTA TGT CTG TAC CAT (DNA bulge)	50.2 [-12.4; -11.0; -9.9]
5'-TGC ACY GTA TGT CTG YAC CAT (ON6)	65.4 [-9.9; 7.2; -7.2]

[a] T_m values (°C) were measured as the maxima of the first derivatives of the thermal melting curves (A_{260} vs. temperature) recorded in medium-salt buffer (100 mM NaCl, 0.1 mM EDTA, 10 mM NaH_2PO_4 , 5 mM Na_2HPO_4 , pH 7.0) with 1.0 μM concentrations of the two complementary strands. ΔT_m values for mismatches are given in brackets in the following order: G:A mismatch, G:G mismatch, G:T mismatch. ΔT_m values were calculated relative to matched duplexes of studied ONs.

monomers **X** and **Y** than in the case of the corresponding DNA*/RNA duplexes.

Because increased thermal stability of the DNA*/DNA duplex containing two bulge-incorporated monomers **Y** (**ON6**) was observed, we decided to study the mismatch discrimination of the central mismatch (position 11 in **ON6**) for this ON (Table 4). The mismatch discrimination capabilities were found to be slightly lower than those of the unmodified 19-mer dsDNA, but sufficient for application as a probe for, for example, nucleic acid detection. A DNA/DNA duplex containing two DNA-T bulges showed high mismatch discrimination (Table 4), thus supporting the trend of destabilization of the terminal parts of the duplex resulting in improved mismatch sensing in the central region.

Monomers **X** and **Y** were incorporated into position 10 (loop region) in the C-rich 22 nt fragment of human telomeric DNA (**ON7**, **ON8**, Table 5). The loop regions of **ON7** and **ON8** (XAA

Table 5. Thermal denaturation temperatures (T_m)^[a] of DNA i-motifs.

Sequence (code)	Conditions	
	Noncrowding	Crowding
5'-CCC TAA CCC TAA CCC TAA CCC T (wt)	45.6	41.1
5'-CCC TAA CCC XAA CCC TAA CCC T (ON7)	39.7	37.9
5'-CCC TAA CCC YAA CCC TAA CCC T (ON8)	43.3	38.3

[a] T_m values (°C) were measured as the minima of the first derivatives of the thermal melting curves (A_{295} vs. temperature) recorded with 3.0 μM concentrations of the strands. Noncrowding conditions: 100 mM KCl, 10 mM sodium cacodylate, pH 5.2. Crowding conditions: 100 mM KCl, 10 mM sodium cacodylate, 20% (v/v) PEG 200, pH 5.2.

and YAA, respectively) are therefore closely structurally related to the native sequence (TAA). The T_m values of the i-motif structures formed by these ONs were studied (Table 5): both monomers **X** and **Y** were found to destabilize the i-motifs at pH 5.2. The T_m values determined under molecular crowding conditions (20% PEG 200), mimicking an intracellular environment, were lower than those under noncrowding conditions, despite the fact that crowding conditions had previously been

shown to induce an i-motif structure.^[27] Nevertheless, destabilization effects of monomers **X** or **Y** were still observed. Generally, the destabilization effect was higher for 3'-linked monomer **X** than for 2'-linked monomer **Y**. The backbone of monomer **Y** is two atoms longer than the that of monomer **X**, and the 2'-linked monomer **Y** can therefore introduce a higher degree of flexibility into the loop region; this possibly makes the i-motif structure more stable than with the 3'-linked monomer **X**. This is in agreement with the previous observations that an increased level of flexibility in the loop regions (positions 4, 10–12 and 16) is favourable for i-motif stability.^[7] On the other hand, the presence of the pyrene moiety in UNA monomers **X** and **Y** led to lower stability of the i-motif structures relative to i-motifs with unmodified UNA incorporations,^[7] presumably due to increased stacking interactions with neighbouring nucleobases leading to structural perturbations of the i-motif loop region, as also indicated by molecular modelling (see the Supporting Information).

Steady-state fluorescence emission studies

The fluorescence properties of oligonucleotides **ON1** and **ON4**, of the corresponding matched duplexes and of duplexes containing single bulges were studied. Steady-state fluorescence emission spectra were recorded at an excitation wavelength of 350 nm. Spectra of single-stranded **ON1**, of duplexes formed between **ON1** and complementary DNA and RNA strands and of duplexes of **ON1** with single-bulge incorporated monomer **X** showed broad emission maxima around 452 nm (Figure 1 A). The fluorescence intensities were similar for single-stranded oligonucleotide **ON1** and its duplex with complementary DNA, whereas an approximately 1.5-fold increase in fluorescence intensity relative to single-stranded **ON1** was observed for the bulge-containing DNA*/DNA duplex of **ON1**. The fluorescence intensities of the matched DNA*/RNA duplex of **ON1** and the DNA*/RNA duplex with a bulge-incorporated monomer **X** were found to be lower than the fluorescence intensity of single-stranded **ON1**. The fluorescence intensity of the bulge-containing duplex was slightly higher than that of the fully matched duplex.

The emission maxima of **ON4**, of its duplexes with complementary DNA and RNA strands and of its duplexes with bulge-incorporated monomer **Y** were observed at approximately 452 nm (Figure 1 B). Although the fluorescence intensities of single-stranded **ON1** and **ON4** were similar, the intensities of all duplexes of **ON4** were significantly lower than that of the single-strand **ON4**. The bulge-containing DNA*/DNA duplex of **ON4** showed higher fluorescence intensity than the fully matched duplex, following the same trend as observed with **ON1**. On the other hand, both the bulge-containing DNA*/RNA duplex of **ON4** and the matched duplex of **ON4** with RNA were found to display similar fluorescence intensities. The observed emission maxima of oligonucleotides **ON1** and **ON4** and of their duplexes originate from an exciplex involving the 5-(pyren-1-yl)uracil unit in monomers **X** and **Y**, which is partially incorporated into the nucleobase stack. Similar results were previously reported with DNA duplexes containing a 5-(pyren-

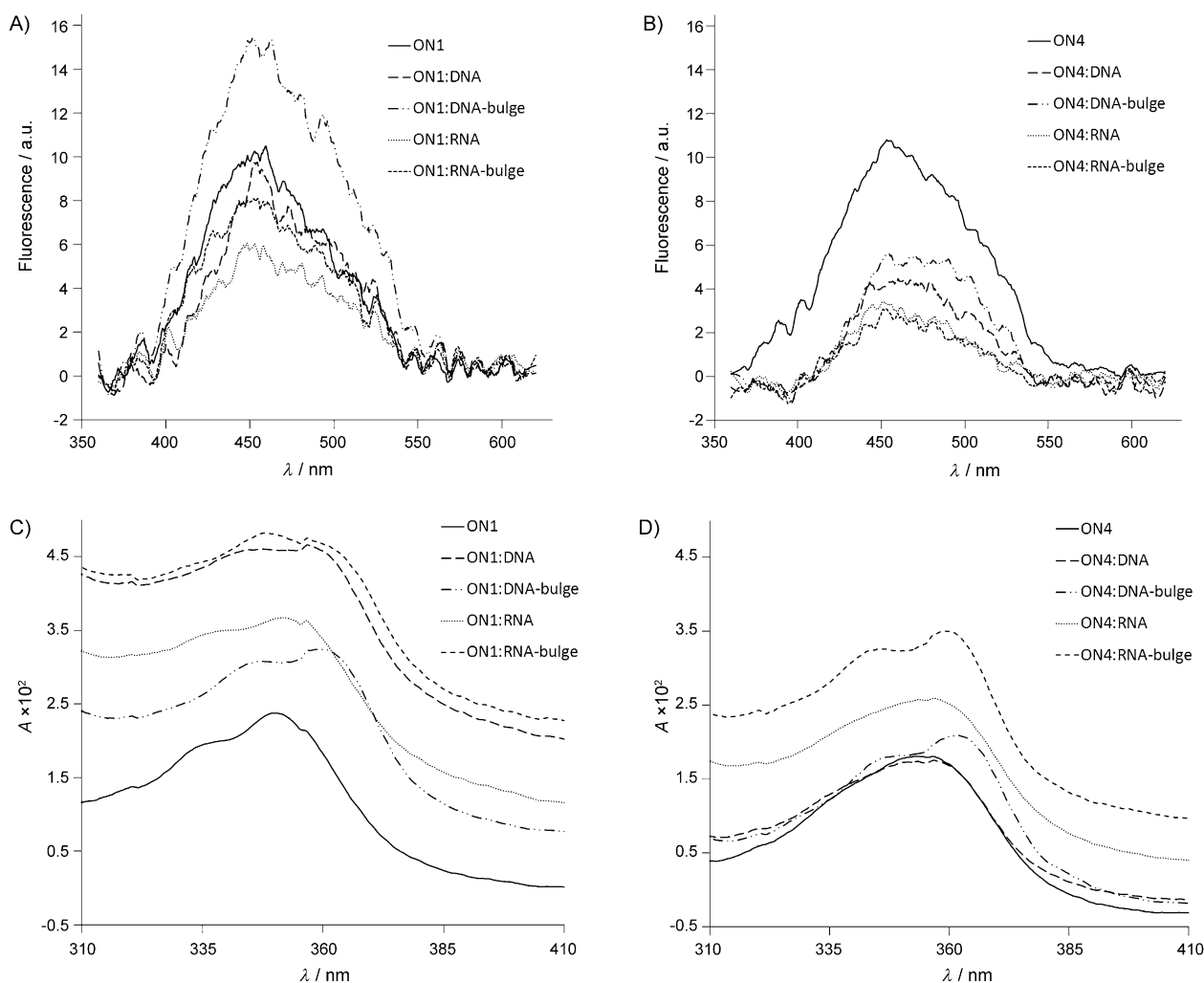


Figure 1. A) Steady-state fluorescence emission spectra of **ON1** in matched duplexes, duplexes containing single bulges and as a single strand. B) Steady-state fluorescence emission spectra of **ON4** in matched duplexes, duplexes containing single bulges and as a single strand. C) Absorption spectrum of **ON1** in matched duplexes, duplexes containing single bulges and as a single strand. D) Absorption spectrum of **ON4** in matched duplexes, duplexes containing single bulges and as a single strand. Measurements were obtained with $1.0 \mu\text{M}$ concentrations of the two strands in medium-salt buffer (100 mM NaCl, 0.1 mM EDTA, 10 mM NaH_2PO_4 , 5 mM Na_2HPO_4 , pH 7.0) at 20°C . $\lambda_{\text{ex}} = 350 \text{ nm}$.

1-yl)-2'-deoxyuridine unit.^[21,23] The variations observed in the fluorescence intensities are probably due to changes in the π -stacking interactions and the electron-transfer reactions between monomers **X** and **Y** and neighbouring nucleobases. The fluorescence intensities of **ON1** and **ON4** were substantially lower than those of ONs containing the 2'-pyrene-modified UNA monomers **W** and **Z**.^[6] On the other hand, due to the direct conjugation of pyrene with a nucleobase, the emission maxima of **ON1** and **ON4** each showed a bathochromic shift of approximately 180 nm in relation to ONs containing 2'-pyrene-modified UNAs.^[6] Larger Stokes shifts of 5-pyrene-modified UNAs might be beneficial for, for example, fluorescence imaging measurements.

Next, fluorescence emission spectra of the i-motif-forming oligonucleotides **ON7** and **ON8** and of their matched DNA*/DNA duplexes were recorded at 350 nm excitation wavelength. The matched duplexes of **ON7** and **ON8** with complementary DNA showed broad emission maxima between 450 and

480 nm and similar fluorescence intensities (Figure 2A and B). The emission maximum of single-stranded **ON7** at pH 7.0 (457 nm) was blue-shifted in relation to that of the matched duplex, whereas its fluorescence intensity was halved. Efficient quenching of fluorescence was observed for **ON7** at pH 5.2 (Figure 2A): the fluorescence of **ON7** at pH 5.2 at 457 nm was quenched by 89% relative to the fluorescence of **ON7** at pH 7.0.

The spectrum of **ON8** at pH 7.0 showed a broad maximum at about 460 nm, whereas at pH 5.2 the fluorescence of **ON8** at 460 nm was quenched by 90% (Figure 2B). It follows that the formation of an i-motif structure under acidic conditions quenches the fluorescence of ONs with 5-(pyren-1-yl)uracilyl UNA monomers in the loop region. One of the possible explanations for this fact is π -stacking interactions or electron-transfer reactions with the neighbouring nucleobases (see molecular modelling in the Supporting Information). Although changes in fluorescence intensities of ONs containing fluores-

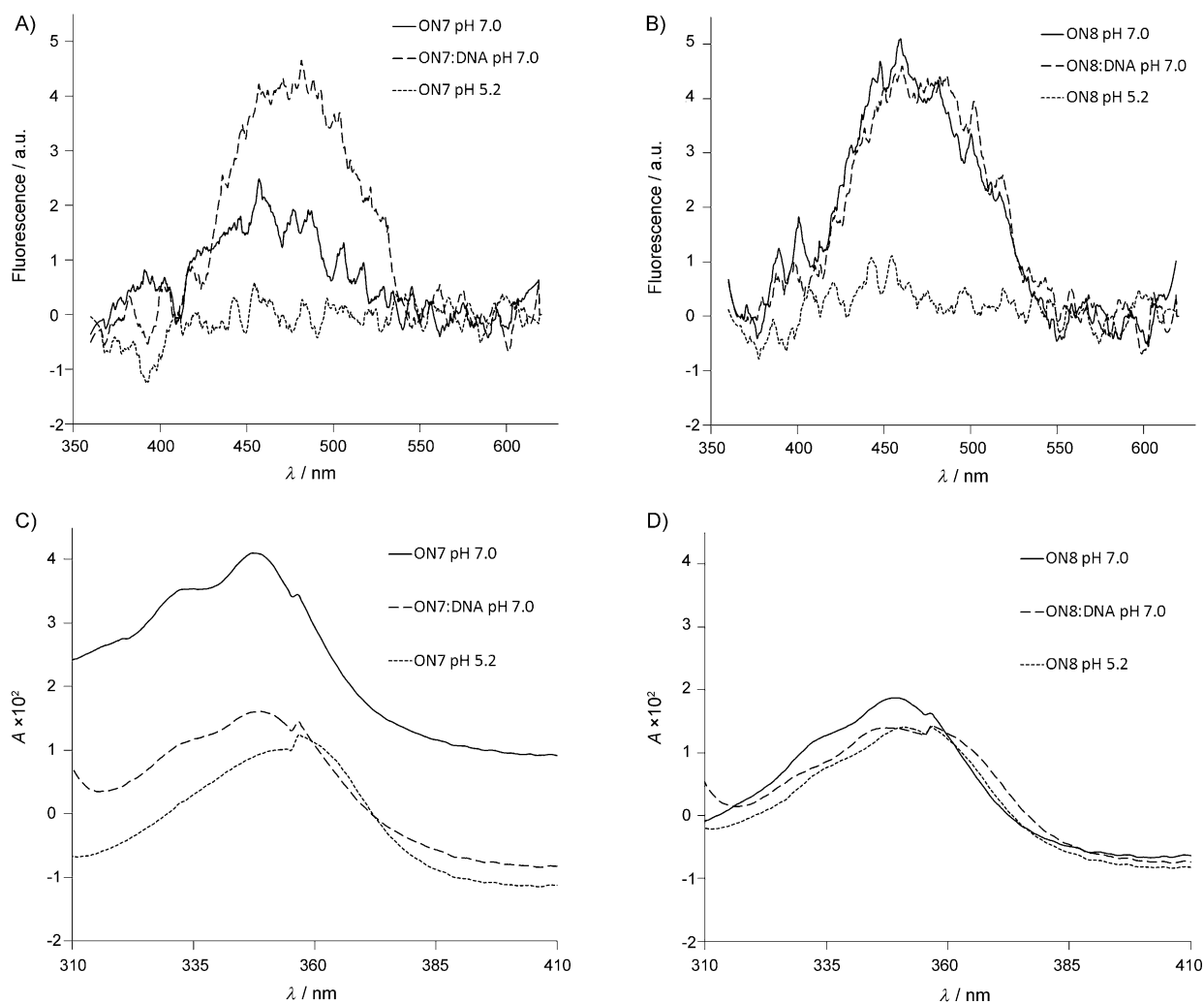


Figure 2. A) Steady-state fluorescence emission spectra of **ON7** in matched duplex (pH 7.0) and as a single strand (pH 7.0 and 5.2). B) Steady-state fluorescence emission spectra of **ON8** in matched duplex (pH 7.0) and as a single strand (pH 7.0 and 5.2). C) Absorption spectrum of **ON7** in matched duplex (pH 7.0) and as a single strand (pH 7.0 and 5.2). D) Absorption spectra of **ON8** in matched duplex (pH 7.0) and as a single strand (pH 7.0 and 5.2). Measurements were obtained with 1.0 μM concentrations of the strands in cacodylate buffer (100 mM KCl, 10 mM sodium cacodylate) at 20 °C. Excitation wavelength: 350 nm.

cently labelled nucleobases have been reported upon formation of an i-motif structure,^[24,28] such efficient quenching of the fluorescence has not previously been observed. Such a dramatic change in fluorescence properties might be caused by strong electronic coupling between the nucleobase and the pyrene moiety in monomers **X** and **Y**, because the two chromophores are linked covalently by a single C–C bond, whereas in the previously reported nucleobase-modified ONs the fluorescent label was attached through an ethylene linker. The efficient quenching of fluorescence upon formation of an i-motif structure might be useful for probing such i-motif structures.

UV/visible absorption studies

In the next part of our study we focused on UV/visible absorption studies of the ONs containing pyrene-modified UNA monomers **X** and **Y**. The UV/visible spectra of oligonucleotides **ON1** and **ON4**, of their duplexes with complementary DNA and RNA

strands and of duplexes containing bulge-incorporated monomers **X** and **Y** were recorded (310–410 nm). **ON1** showed an absorption maximum at 350 nm, as typically observed for a pyrenyl group (Figure 1C). Shoulders at 335 and 356 nm were also observed. The duplexes of **ON1** with complementary DNA and RNA both showed slightly broader absorptions in the 340–360 nm region, and the A_{350}/A_{356} ratios were slightly decreased, thus indicating small bathochromic shifts in the absorption spectra, presumably due to partial intercalation of the uracil part of the 5-(pyren-1-yl)uracil moiety into the base stack. The DNA*/DNA duplex of **ON1** containing bulge-incorporated monomer **X** showed two local absorption maxima at 345 and 360 nm. Notably, the 10 nm shift of the absorption maximum of the pyrene unit to 360 nm indicates that the pyrene moiety in the bulge intercalates into the DNA*/DNA duplex. Local absorption maxima of the DNA*/RNA duplex of **ON1** containing bulge-incorporated monomer **X** were located at 347 and 356 nm. The bathochromic shift of the pyrene ab-

sorption maximum in the bulge-containing DNA*/RNA duplex was less profound than in the DNA*/DNA duplex, presumably due to the fact that the intercalation into DNA/RNA duplex is more demanding and less favourable.

The same trend was observed when the UV/visible absorption of **ON4** and of its duplexes were studied. Single-stranded **ON4** and duplexes of **ON4** with complementary DNA and RNA showed absorption maxima at approximately 353 nm (Figure 1D). On the other hand, absorption maxima and duplexes of **ON4** containing bulges were found to be around 345 and 360 nm, thus implying significant bathochromic shifts.

In summary, these results indicate that bulge-incorporated UNA monomers containing pyrene-modified nucleobases are able to intercalate into both DNA/DNA and DNA/RNA duplexes, with the pyrene moieties being located in the major grooves in the matched duplexes of two ONs of identical nucleotide length.

The UV/visible absorption properties of the i-motif-forming oligonucleotides **ON7** and **ON8** were also studied. At pH 7.0 **ON7** and **ON8** each showed the typical absorption maximum for single-stranded ONs containing pyrene-modified UNA monomers at approximately 350 nm (Figure 2C, 2D). At pH 5.2, however, small bathochromic shifts of the absorption maxima of **ON7** and **ON8** were observed. These shifts indicate stacking interactions between the pyrene-modified nucleobases and the neighbouring nucleobases when i-motif structures are present at pH 5.2. More intensive stacking was indicated for the 3'-linked monomer **X**, presumably due to the expected lower flexibility of the loop region of the i-motif for **ON7** (containing monomer **X**) relative to **ON8**.

Conclusions

We have developed a synthesis of two new phosphoramidites suitable for incorporation of 5-(pyren-1-yl)uracilyl UNA monomers **X** and **Y** into ONs. Monomers **X** and **Y** were found to destabilize i-motif structures at pH 5.2, both under molecular crowding and noncrowding conditions. The presence of one or two of these pyrene-modified UNA monomers in a DNA strand led to decreases in the thermal stabilities of DNA*/DNA and DNA*/RNA duplexes, but the duplex thermal stabilities were higher than those of previously reported^[6] duplexes containing unmodified UNA monomers (**U**), presumably due to major groove interactions of the pyrene moiety. The mismatch discrimination of **ON1–6** varied from low to high depending on the relative positioning of monomers within the duplexes. The presence of two bulge-incorporated pyrene-modified UNA monomers **Y** (nine bases apart) was able to stabilize a DNA*/DNA duplex relative to the unmodified matched duplex. In general, however, the thermal stabilities of DNA*/DNA and DNA*/RNA duplexes containing bulge-incorporated pyrene-modified monomers were similar to or slightly lower than those of unmodified matched duplexes, but thus significantly better than those of matched duplexes containing **X** and **Y** monomers. From UV/visible absorption studies we conclude that bulge-incorporated UNA monomers containing pyrene-modified nucleobases intercalate into both DNA/DNA and

DNA/RNA duplexes. The discovery that monomer **Y** can have either stabilizing or destabilizing effects in nucleic acid duplexes, depending on the way in which it is incorporated, might be useful for the design of antisense ONs and hybridization probes. Steady-state fluorescence emission studies of ONs with single incorporation of pyrene-modified monomers **X** and **Y** in most cases revealed decreases in fluorescence intensity upon hybridization to DNA or RNA. Efficient quenching of the fluorescence of i-motif-forming ONs containing pyrene-modified UNA monomers was observed at pH 5.2. To the best of our knowledge this is so far the most effective fluorescence quenching upon formation of an i-motif structure.

Experimental Section

NMR spectra were recorded with a 400 MHz (¹H at 400 MHz, ¹³C at 110.6 MHz, ³¹P at 162 MHz) spectrometer in CDCl₃ solutions. Chemical shifts are reported in ppm relative to TMS (¹H, internal standard, δ_{H} TMS = 0.00 ppm), solvent peaks (¹³C, internal standard, δ_{C} CDCl₃ = 77.00 ppm), or 85% H₃PO₄ (³¹P, external standard, δ_{P} 85% H₃PO₄ = 0.00 ppm). Assignments of the NMR signals are based on 2D correlation experiments. High-resolution MS spectra were collected by use of electrospray ionization. ONs were synthesized with an ÄKTA oligopilot Plus system (GE Healthcare Life Sciences), and the compositions of ONs were confirmed by MALDI-MS (Microflex MALDI-TOF MS, Bruker Daltonics) and by their purities (> 90%) by ion-exchange HPLC.

5'-O-(4,4'-Dimethoxytrityl)-5-iodo-2',3'-secouridine (2): 5-Iodo-uridine^[25] (1, 3.15 g, 4.69 mmol) was dissolved in a mixture of 1,4-dioxane (60 mL) and water (12 mL). A solution of NaIO₄ (1.10 g, 5.16 mmol) in water (10 mL) was added, and the reaction mixture was stirred for 1 h at RT. 1,4-Dioxane (50 mL) was then added, and stirring was continued for 15 min. The precipitate was filtered off and washed with 1,4-dioxane (25 mL). NaBH₄ (203 mg, 5.34 mmol) was added to the filtrate, and the mixture was stirred for 1 h at RT. A mixture of acetic acid and pyridine (6 mL, 1:1, v/v) was then added, and the resulting mixture was concentrated under reduced pressure to a volume of approximately 25 mL. CH₂Cl₂ (50 mL) was added to this solution, and washing was performed with saturated aqueous NaHCO₃ (50 mL). The separated organic phase was dried over MgSO₄ and, after filtration, concentrated to dryness under reduced pressure. The residue was purified by silica gel column chromatography (0–2.5% MeOH in CH₂Cl₂, v/v) to furnish nucleoside **2** (2.28 g, 72%) as a white foam. ¹H NMR (400 MHz, CDCl₃): δ = 3.08 (dd, $J_{\text{gem}} = 10.4$ Hz, $J_{5',a,4'} = 6.1$ Hz, 1H; H-5'a), 3.18 (dd, $J_{\text{gem}} = 10.4$ Hz, $J_{5',b,4'} = 3.7$ Hz, 1H; H-5'b), 3.64–3.82 (m, 11H; H-2',3',4', OCH₃), 5.95 (t, $J_{1',2'} = 5.3$ Hz, 1H; H-1'), 6.74–6.82 (m, 4H; H-3-PhOMe), 7.12–7.27 (m, 7H; H-*o,p*-Ph, H-2-PhOMe), 7.29–7.35 (m, 2H; H-*m*-Ph), 7.79 ppm (s, 1H; H-6); ¹³C NMR (100.6 MHz, CDCl₃): δ = 55.24 (OCH₃), 62.90, 63.49, 63.65 (CH₂-2', CH₂-3', CH₂-5'), 69.18 (C-5), 81.83 (CH-4'), 85.93 (CH-1'), 86.58 (CPh(PhOMe)₂), 113.25 (CH-3-PhOMe), 126.92 (CH-*p*-Ph), 127.92 (CH-*o,m*-Ph), 129.84 and 129.89 (CH-2-PhOMe), 135.41 and 135.54 (C-1-PhOMe), 144.31 (C-*i*-Ph), 144.90 (CH-6), 150.92 (C-2), 158.47 (C-4-PhOMe), 160.51 ppm (C-4); HRMS (ESI): m/z calcd for C₃₀H₃₁IN₂NaO₈: 697.1017 [M+Na]⁺; found: 697.0994.

2'-O-Benzoyl-5'-O-(4,4'-dimethoxytrityl)-5-iodo-2',3'-secouridine (3): A solution of nucleoside **2** (645 mg, 0.95 mmol) and DBU (286 μ L, 1.91 mmol) in anhydrous CH₂Cl₂ (25 mL) was cooled to –78 °C, and a solution of benzoyl chloride in CH₂Cl₂ (0.5 M, 2.00 mL, 1.00 mmol) was added dropwise over a period of 20 min.

The reaction mixture was stirred at -78°C for 30 min. MeOH (0.9 mL) was then added, and the mixture was allowed to warm to RT. The mixture was extracted with saturated aqueous NaHCO_3 (50 mL). The separated organic phase was dried over MgSO_4 and, after filtration, was concentrated to dryness under reduced pressure. The crude product was purified by high-performance FLASH chromatography (HPFC) on SiO_2 (0–53% EtOAc in petroleum ether) to furnish benzoate **3** (522 mg, 70%) as a white foam. ^1H NMR (400 MHz, CDCl_3): $\delta = 3.12$ (dd, $J_{\text{gem}} = 10.6$ Hz, $J_{5'a,4'} = 6.0$ Hz, 1H; H-5'a), 3.23 (dd, $J_{\text{gem}} = 10.6$ Hz, $J_{5'b,4'} = 4.0$ Hz, 1H; H-5'b), 3.69–3.82 (m, 9H; H-3',4', OCH_3), 4.44 (dd, $J_{\text{gem}} = 11.9$ Hz, $J_{2'a,1'} = 4.5$ Hz, 1H; H-2'a), 4.63 (dd, $J_{\text{gem}} = 11.9$ Hz, $J_{2'b,1'} = 4.5$ Hz, 1H; H-2'b), 6.20 (t, $J_{1',2'} = 4.5$ Hz, 1H; H-1'), 6.77–6.81 (m, 4H; H-3-PhOMe), 7.15–7.33 (m, 7H; H-*o,p*-Ph, H-2-PhOMe), 7.30–7.34 (m, 2H; H-*m*-Ph), 7.43–7.48 (m, 2H; H-*m*-Bz), 7.57–7.61 (m, 1H; H-*p*-Bz), 7.84 (s, 1H; H-6), 7.96–8.00 (m, 2H; H-*o*-Bz), 8.95 ppm (brs, 1H; NH); ^{13}C NMR (100.6 MHz, CDCl_3): $\delta = 55.23$ (OCH_3), 62.38 ($\text{CH}_2\text{-5}'$), 63.39 ($\text{CH}_2\text{-3}'$), 64.21 ($\text{CH}_2\text{-2}'$), 68.72 (C-5), 82.42 (CH-4'), 83.30 (CH-1'), 86.73 (CPh(PhOMe) $_2$), 113.27 (CH-3-PhOMe), 126.95 (CH-*p*-Ph), 127.88 (CH-Ar), 127.97 (CH-Ar), 128.71 (CH-Ar), 128.82 (CH-Ar), 129.76 (CH-Ar), 129.82 (CH-Ar), 129.87 (CH-Ar), 133.69 (CH-*p*-Bz), 135.24 and 135.39 (C-1-PhOMe), 144.21 (C-*i*-Ph), 144.39 (CH-6), 149.91 (C-2), 158.53 (C-4-PhOMe), 159.67 (C-4), 171.17 ppm (C=O benzoyl). HRMS (ESI): m/z calcd for $\text{C}_{37}\text{H}_{35}\text{I}_2\text{N}_2\text{NaO}_9$: 801.1279 $[M+\text{Na}]^+$; found: 801.1288.

2'-O-Benzoyl-5'-O-(4,4'-dimethoxytrityl)-5-(pyren-1-yl)-2',3'-secouridine (4): A nitrogen-purged mixture of benzoate **3** (150 mg, 0.19 mmol), pyrene-1-boronic acid (142 mg, 0.58 mmol), sodium carbonate (61 mg, 0.58 mmol), PPh_3 (10 mg, 39 μmol) and $\text{Pd}(\text{OAc})_2$ (4.3 mg, 19 μmol) in toluene (4.5 mL) and water (675 μL) was stirred at 100°C for 1 h. After the system had cooled, volatiles were removed under reduced pressure. The residue was dissolved in CH_2Cl_2 (20 mL) and washed with water (30 mL). The organic phase was dried over MgSO_4 and, after filtration, was concentrated to dryness under reduced pressure. The residue was dissolved in CH_2Cl_2 and coevaporated with silica gel. The product was purified by silica gel column chromatography (0–1% MeOH in CH_2Cl_2) to furnish compound **4** (58 mg, 35%) as a yellowish amorphous solid. ^1H NMR (400 MHz, CDCl_3): $\delta = 3.14$ (dd, $J_{\text{gem}} = 10.2$ Hz, $J_{5'a,4'} = 6.0$ Hz, 1H; H-5'a), 3.26 (dd, $J_{\text{gem}} = 10.2$ Hz, $J_{5'b,4'} = 5.0$ Hz, 1H; H-5'b), 3.51, 3.54 (2s, 3H; OCH_3), 3.64–3.73 (m, 1H; H-3'a), 3.78–3.86 (m, 1H; H-3'b), 3.91–3.98 (m, 1H; H-4'), 4.57 (dd, $J_{\text{gem}} = 11.8$ Hz, $J_{2'a,1'} = 4.6$ Hz, 1H; H-2'a), 4.75 (dd, $J_{\text{gem}} = 11.8$ Hz, $J_{2'b,1'} = 4.9$ Hz, 1H; H-2'b), 6.38 (t, $J_{1',2'} = 4.7$ Hz, 1H; H-1'), 6.51–6.64 (m, 4H; H-3-PhOMe), 7.09–7.37 (m, 14H; H-Ph, H-2-PhOMe, H-Bz), 7.64 (s, 1H; H-6), 7.91–8.25 (m, 9H; H-pyrene), 8.78 ppm (brs, 1H; NH); ^{13}C NMR (100.6 MHz, CDCl_3): $\delta = 54.99$ (OCH_3), 62.89 ($\text{CH}_2\text{-3}'$), 63.25 ($\text{CH}_2\text{-5}'$), 64.14 ($\text{CH}_2\text{-2}'$), 82.17 (CH-4'), 83.25 (CH-1'), 86.65 (CPh(PhOMe) $_2$), 113.07 and 113.13 (CH-3-PhOMe), 124.17 (C-Ar), 124.57 (CH-Ar), 124.81 (C-Ar), 125.30 (CH-Ar), 125.41 (CH-Ar), 126.07 (CH-Ar), 126.89 (CH-Ar), 127.22 (CH-Ar), 127.67 (CH-Ar), 127.89 (CH-Ar), 128.19 (C-Ar), 128.59 (CH-Ar), 128.86 (C-Ar), 129.75 (CH-Ar), 129.79 (CH-Ar), 129.84 (CH-Ar), 130.73 (C-Ar), 131.17 (C-Ar), 133.61 (C-Ar), 135.10 (C-Ar), 135.49 (C-Ar), 137.37 (CH-6), 144.56 (C-*i*-Ph), 150.20 (C-2), 158.46 (C-4-PhOMe), 161.94 (C-4), 166.00 ppm (C=O benzoyl); HRMS (ESI): m/z calcd for $\text{C}_{53}\text{H}_{44}\text{N}_2\text{NaO}_9$: 875.2939 $[M+\text{Na}]^+$; found: 875.2966.

2'-O-Benzoyl-3'-O-[2-cyanoethoxy(diisopropylamino)phosphino]-5'-O-(4,4'-dimethoxytrityl)-5-(pyren-1-yl)-2',3'-secouridine (5): Nucleoside **4** (142 mg, 0.17 mmol) was stirred with anhydrous DIPEA (0.67 mmol) in anhydrous CH_2Cl_2 (10 mL), and 2-cyanoethyl-*N,N*-diisopropylchlorophosphoramidite [$\text{P}(\text{Cl})(\text{NiPr}_2)(\text{OCH}_2\text{CH}_2\text{CN})$, 56 μL , 0.25 mmol] was added. The mixture was stirred under N_2 at RT for 2 h. Further $\text{P}(\text{Cl})(\text{NiPr}_2)(\text{OCH}_2\text{CH}_2\text{CN})$ (56 μL , 0.25 mmol) was then

added, and stirring was continued for another 2 h. The reaction was quenched by addition of MeOH (0.5 mL), and the resulting mixture was stirred for another 5 min. The solution was diluted with CH_2Cl_2 (10 mL) and washed with saturated aqueous NaHCO_3 (15 mL). The organic phase was dried over MgSO_4 and, after filtration, was concentrated to dryness under reduced pressure. The residue was dissolved in EtOAc (2 mL) and added dropwise to ice-cold petroleum ether (100 mL). The precipitate was filtered off and dried under vacuum. Phosphoramidite **5** (163 mg, 93%) was obtained as an off-white solid. ^{31}P NMR (162 MHz, CDCl_3): $\delta = 148.65$ and 149.06 ppm; HRMS (ESI): m/z calcd for $\text{C}_{62}\text{H}_{61}\text{N}_4\text{NaO}_{10}\text{P}$: 1075.4018 $[M+\text{Na}]^+$; found: 1075.3987.

3'-O-(tert-Butyldimethylsilyl)-5'-O-(4,4'-dimethoxytrityl)-5-iodo-2',3'-secouridine (6): Nucleoside **3** (511 mg, 0.66 mmol) was co-evaporated with anhydrous pyridine (2 \times 5 mL). The residue was dissolved in anhydrous pyridine (10 mL), and TBSCl (593 mg, 3.94 mmol) was added. The reaction mixture was stirred at RT overnight. Water (5 mL) was then added, and stirring was continued for 20 min at RT. The resulting mixture was diluted with MeOH (50 mL), after which sodium hydroxide (735 mg, 18.37 mmol) was added. The reaction mixture was stirred at RT for 2 h. The mixture was then diluted with CH_2Cl_2 (30 mL) and washed with saturated aqueous NH_4Cl (30 mL). The organic phase was dried over MgSO_4 and, after filtration, was concentrated to dryness under reduced pressure. Purification by silica gel column chromatography (20–30% EtOAc in petroleum ether) afforded compound **6** (394 mg, 76%) as a white foam. ^1H NMR (400 MHz, CDCl_3): $\delta = 0.06$ (s, 6H; 2SiCH $_3$), 0.88 (s, 9H; C(CH $_3$) $_3$), 3.09 (dd, $J_{\text{gem}} = 10.6$ Hz, $J_{5'a,4'} = 6.1$ Hz, 1H; H-5'a), 3.18 (dd, $J_{\text{gem}} = 10.5$ Hz, $J_{5'b,4'} = 3.9$ Hz, 1H; H-5'b), 3.62–3.78 (m, 5H; 2H-3', 2H-2', H-4'), 3.79 (s, 6H; 2OCH $_3$), 5.90 (dd, $J_{1',2'a} = 5.8$ Hz, $J_{1',2'b} = 4.0$ Hz, 1H; H-1'), 6.79–6.83 (m, 4H; H-3-PhOMe), 7.17–7.37 (m, 9H; H-Ph, H-2-PhOMe), 7.83 (s, 1H; H-6), 8.77 ppm (brs, 1H; NH); ^{13}C NMR (100.6 MHz, CDCl_3): $\delta = -5.50$ (SiCH $_3$), 18.28 (C(CH $_3$) $_3$), 25.82 (C(CH $_3$) $_3$), 55.25 (OCH $_3$), 63.46, 63.52, 63.92 ($\text{CH}_2\text{-2}'$, $\text{CH}_2\text{-3}'$, $\text{CH}_2\text{-5}'$), 68.23 (C-5), 81.85 (CH-4'), 85.39 (CH-1'), 86.64 (CPh(PhOMe) $_2$), 113.24 (CH-3-PhOMe), 126.91 (CH-4-Ph), 127.92 (CH-2,3-Ph), 129.84 and 129.90 (CH-2-PhOMe), 135.50 and 135.61 (C-1-PhOMe), 144.39 (C-1-Ph), 144.93 (CH-6), 150.02 (C-2), 158.53 (C-4-PhOMe), 159.81 ppm (C-4); HRMS (ESI): m/z calcd for $\text{C}_{36}\text{H}_{45}\text{I}_2\text{N}_2\text{NaO}_8\text{Si}$: 811.1882 $[M+\text{Na}]^+$; found: 811.1914.

3'-O-(tert-Butyldimethylsilyl)-5'-O-(4,4'-dimethoxytrityl)-5-(pyren-1-yl)-2',3'-secouridine (7): Nucleoside **7** was prepared as described for compound **4**; nucleoside **6** (350 mg, 0.44 mmol), pyrene-1-boronic acid (328 mg, 1.33 mmol), $\text{Pd}(\text{OAc})_2$ (10 mg, 44 μmol), PPh_3 (23 mg, 89 μmol) and Na_2CO_3 (141 mg, 1.33 mmol) in toluene (13 mL) and water (1.95 mL) were used. Purification by silica gel column chromatography (0–0.75% MeOH in CH_2Cl_2) afforded nucleoside **7** (220 mg, 57%) as a yellowish amorphous solid. ^1H NMR (400 MHz, CDCl_3): $\delta = 0.05$ (s, 6H; 2SiCH $_3$), 0.87 (s, 9H; C(CH $_3$) $_3$), 3.00–3.15 (m, 2H; H-5'a, 2'-OH), 3.20 (dd, $J_{\text{gem}} = 9.7$ Hz, $J_{5'b,4'} = 4.1$ Hz, 1H; H-5'b), 3.50, 3.53 (2s, OCH $_3$), 3.65 (dd, $J_{\text{gem}} = 10.8$ Hz, $J_{3'a,4'} = 7.4$ Hz, 1H; H-3'a), 3.68–4.00 (m, 4H; 2H-2', H-3'b, H-4'), 6.09 (t, $J_{1',2'} = 4.4$ Hz, 1H; H-1'), 6.45–6.64 (m, 4H; H-3-PhOMe), 7.09–7.22 (m, 7H; DMT), 7.30–7.36 (m, 2H; DMT), 7.45 (td, $J_1 = 7.4$ Hz, $J_2 = 2.9$ Hz, 1H; H-pyrene), 7.50–7.56 (m, 1H; H-pyrene), 7.60–7.71 (m, 3H; H-6, H-pyrene), 7.91–8.11 (m, 4H; H-pyrene), 8.16 (d, $J = 7.4$ Hz, 1H; H-pyrene), 8.86 ppm (brs, 1H; NH); ^{13}C NMR (100.6 MHz, CDCl_3): $\delta = -5.49$ (SiCH $_3$), 18.29 (C(CH $_3$) $_3$), 25.82 (C(CH $_3$) $_3$), 54.97 (OCH $_3$), 63.24 ($\text{CH}_2\text{-5}'$), 63.57 ($\text{CH}_2\text{-3}'$), 64.13 ($\text{CH}_2\text{-2}'$), 82.07 (CH-4'), 85.58 (CH-1'), 86.50 (CPh(PhOMe) $_2$), 113.01 and 113.06 (CH-3-PhOMe), 124.27 (CH-Ar), 124.51 (CH-Ar), 124.57 (CH-Ar), 124.84 (CH-Ar), 125.15 (CH-Ar), 125.23 (CH-Ar), 125.96 (CH-Ar), 126.82 (CH-Ar),

127.21 (CH-Ar), 127.67 (CH-Ar), 127.84 (CH-Ar), 128.34 (CH-Ar), 128.42 (CH-Ar), 128.54 (CH-Ar), 129.56 (CH-Ar), 129.79 (CH-Ar), 129.88 (CH-Ar), 130.72 (CH-Ar), 131.15 (CH-Ar), 131.90 (CH-Ar), 131.92 (CH-Ar), 132.04 (CH-Ar), 132.13 (CH-Ar), 135.26 (C-Ar), 135.66 (C-Ar), 140.30 (C-6), 144.73 (C-*i*-Ph), 150.32 (C-2), 158.42 ppm (C-4-PhOMe); HRMS (ESI): m/z calcd for $C_{52}H_{54}N_2NaO_8Si$: 885.3542 $[M+Na]^+$; found: 885.3518.

3'-O-(tert-Butyldimethylsilyl)-3'-O-[2-cyanoethoxy(diisopropylamino)phosphino]-5'-O-(4,4'-dimethoxytrityl)-5-(pyren-1-yl)-2',3'-secouridine (8): Phosphoramidite **8** was prepared as described for compound **5**; nucleoside **7** (200 mg, 0.23 mmol), DIPEA (161 μ L, 0.93 mmol) and P(Cl)(N i Pr $_2$)(OCH $_2$ CH $_2$ CN) (155 μ L, 0.70 mmol) in anhydrous CH $_2$ Cl $_2$ (16 mL) were used. Phosphoramidite **8** (159 mg, 65 μ mol) was obtained as an off-white solid. ^{31}P NMR (162 MHz, CDCl $_3$): δ = 149.47 ppm; HRMS (ESI): m/z calcd for $C_{61}H_{71}N_4NaO_9PSi$: 1085.4620 $[M+Na]^+$; found: 1085.4614.

Oligonucleotide synthesis and purification: Synthesis of ONs was performed on 1 μ mol scale with an automated DNA synthesizer. Standard cycle procedures were applied for unmodified phosphoramidites as well as for amidites **5** and **8** with use of a solution of 1*H*-tetrazole (0.45 M) as an activator. Stepwise coupling yields, as determined by a spectrophotometric DMT $^+$ assay, were above 99% for phosphoramidites **5** and **8** (20 min coupling time) and unmodified DNA phosphoramidites (2 min coupling time). Removal of the nucleobase protecting groups and cleavage from solid support was effected under standard conditions (32% aqueous ammonia, 12 h, 55 $^{\circ}$ C). Removal of the TBS group to obtain **ON4-6** and **ON8** was accomplished by treatment with Et $_3$ N \cdot 3HF in *N*-methyl-2-pyrrolidone in the presence of Et $_3$ N (4 h, 67 $^{\circ}$ C) and was followed by detritylation (80% AcOH, 30 min, RT). **ON1**, **ON4**, **ON7** and **ON8** were precipitated from acetone after detritylation. **ON2** and **ON3** were purified by DMT-ON RP-HPLC with a C18-column, followed by detritylation and acetone precipitation. **ON5** and **ON6** were purified by DMT-OFF ion-exchange HPLC, followed by acetone precipitation. Analysis by ion-exchange HPLC verified the purity of all oligonucleotides to be >90%, and their compositions were verified by MALDI-TOF mass spectrometry (Table 6).

Table 6. MALDI-MS analysis of ON1-8.

Code	Sequence	M_{calcd}	M_{found}
ON1	5'-TGC ACT GTA XGT CTG TAC CAT	6591.4	6591.3
ON2	5'-TGC ACT GTA XGX CTG TAC CAT	6795.6	6797.0
ON3	5'-TGC ACX GTA TGT CTG XAC CAT	6795.6	6797.0
ON4	5'-TGC ACT GTA YGT CTG TAC CAT	6591.4	6592.2
ON5	5'-TGC ACT GTA YGY CTG TAC CAT	6795.6	6795.5
ON6	5'-TGC ACY GTA TGT CTG YAC CAT	6795.6	6799.8
ON7	5'-CCC TAA CCC XAA CCC TAA CCC T	6708.5	6709.9
ON8	5'-CCC TAA CCC YAA CCC TAA CCC T	6708.5	6712.2

Thermal denaturation studies of nucleic acid duplexes: Concentrations of ONs were calculated by use of extinction coefficients,^[29] including that of the 5-(pyren-2-yl)uracil moiety.^[23] ONs (1.0 μ M of each strand) were mixed in medium-salt buffer [NaCl (100 mM), EDTA (0.1 mM), NaH $_2$ PO $_4$ (10 mM), Na $_2$ HPO $_4$ (5 mM), pH 7.0], and the resulting mixtures were each heated to 90 $^{\circ}$ C (10 min) and allowed to cool slowly to the starting temperature of the experiment (20 $^{\circ}$ C). Thermal denaturation temperatures (T_m) were determined with a Beckman DU 800 spectrophotometer as the maxima of the

first derivatives of the thermal denaturation curves (A_{260} vs. T). Reported T_m values are averages of two measurements within ± 1.0 $^{\circ}$ C.

Thermal denaturation studies of i-motifs: Concentrations of ONs were calculated by use of extinction coefficients,^[29] including that of the 5-(pyren-2-yl)uracil moiety.^[23] ONs (3.0 μ M) were mixed either in sodium cacodylate buffer [KCl (100 mM), sodium cacodylate (10 mM), pH 5.2] or in sodium cacodylate buffer with PEG 200 [KCl (100 mM), sodium cacodylate (10 mM), PEG 200 (20%, v/v), pH 5.2], and the resulting mixtures were heated to 90 $^{\circ}$ C (10 min) and then allowed to cool slowly to the starting temperature of the experiment (15 $^{\circ}$ C). Thermal denaturation temperatures (T_m) were determined with a Beckman DU 800 spectrophotometer as the minima of the first derivatives of the thermal denaturation curves (A_{295} vs. temperature). Reported T_m values are averages of two measurements within ± 1.0 $^{\circ}$ C.

Steady-state fluorescence emission spectra: ONs were thoroughly mixed either in medium-salt buffer [NaCl (100 mM), EDTA (0.1 mM), NaH $_2$ PO $_4$ (10 mM), Na $_2$ HPO $_4$ (5 mM), pH 7.0] or in sodium cacodylate buffer [KCl (100 mM), sodium cacodylate (10 mM), pH 5.2 or pH 7.0] in concentrations of 1 μ M of each strand. The samples were heated at 90 $^{\circ}$ C for 10 min and allowed to cool slowly to 20 $^{\circ}$ C before measurements in quartz optical cells with a path length of 1.0 cm. Background spectra of buffer solutions were recorded with an excitation wavelength of 350 nm and were subtracted from the relevant spectra. Steady-state spectra (360–620 nm) were recorded with a PerkinElmer LS 55 luminescence spectrometer at 20 $^{\circ}$ C as averages of three scans with use of an excitation wavelength of 350 nm, an excitation slit of 4.0 nm, an emission slit of 2.5 nm and a scan speed of 120 nm min $^{-1}$.

Acknowledgements

Funding from The University of Southern Denmark and The European Research Council under The European Union's Seventh Framework Programme (FP7/2007–2013)/ERC Grant agreement No. 268776 is gratefully acknowledged.

Keywords: fluorescence · i-motifs · nucleic acid hybridization · oligonucleotides · unlocked nucleic acids

- [1] For reviews see: a) A. Pasternak, J. Wengel, *Org. Biomol. Chem.* **2011**, *9*, 3591–3597; b) H. Doessing, B. Vester, *Molecules* **2011**, *16*, 4511–4526; c) M. A. Campbell, J. Wengel, *Chem. Soc. Rev.* **2011**, *40*, 5680–5689.
- [2] P. Nielsen, L. H. Dreijøe, J. Wengel, *Bioorg. Med. Chem.* **1995**, *3*, 19–28.
- [3] N. Langkjær, A. Pasternak, J. Wengel, *Bioorg. Med. Chem.* **2009**, *17*, 5420–5425.
- [4] T. B. Jensen, N. Langkjær, J. Wengel, *Nucleic Acids Symp. Ser.* **2008**, *52*, 133–134.
- [5] A. Pasternak, J. Wengel, *Nucleic Acids Res.* **2010**, *38*, 6697–6706.
- [6] K. K. Karlsen, A. Pasternak, T. B. Jensen, J. Wengel, *ChemBioChem* **2012**, *13*, 590–601.
- [7] A. Pasternak, J. Wengel, *Bioorg. Med. Chem. Lett.* **2011**, *21*, 752–755.
- [8] T. Agarwal, S. Kumar, S. Maiti, *Biochimie* **2011**, *93*, 1694–1700.
- [9] M. M. Mangos, K.-L. Min, E. Viazovkina, A. Galarneau, M. I. Elzagheid, M. A. Parniak, M. J. Damha, *J. Am. Chem. Soc.* **2003**, *125*, 654–661.
- [10] A. Muñoz-Alarcón, P. Guterstam, C. Romero, M. A. Behlke, K. A. Lennox, J. Wengel, S. El Andaloussi, Ü. Langel, *ISRN Pharm.* **2012**, *2012*, 407154.
- [11] a) J. B. Bramsen, M. B. Laursen, A. F. Nielsen, T. B. Hansen, C. Bus, N. Langkjær, B. R. Babu, T. Højland, M. Abramov, A. Van Aerschot, D. Odadzic, R. Smicic, J. Haas, C. Andree, J. Barman, M. Wenska, P. Srivastava, C. Zhou, D. Honcharenko, S. Hess, E. Muller, G. V. Bobkov, S. N. Mikhailov, E.

- Fava, T. F. Meyer, J. Chattopadhyaya, M. Zerial, J. W. Engels, P. Herdewijn, J. Wengel, J. Kjems, *Nucleic Acids Res.* **2009**, *37*, 2867–2881; b) D. M. Kenski, A. J. Cooper, J. J. Li, A. T. Willingham, H. J. Haringsma, T. A. Young, N. A. Kuklin, J. J. Jones, M. T. Cancilla, D. R. McMasters, M. Mathur, A. B. Sachs, W. M. Flanagan, *Nucleic Acids Res.* **2010**, *38*, 660–671; c) M. B. Laursen, M. M. Pakula, S. Gao, K. Fluiter, O. R. Mook, F. Baas, N. Langkjær, S. L. Wengel, J. Wengel, J. Kjems, J. B. Bramsen, *Mol. BioSyst.* **2010**, *6*, 862–870; d) D. Werk, J. Wengel, S. L. Wengel, H.-P. Grunert, H. Zeichhardt, J. Kurreck, *FEBS Lett.* **2010**, *584*, 591–598; e) N. Vaish, F. Chen, S. Seth, K. Fosnaugh, Y. Liu, R. Adami, T. Brown, Y. Chen, P. Harvie, R. Johns, G. Severson, B. Granger, P. Charmley, M. Houston, M. V. Templin, B. Polisky, *Nucleic Acids Res.* **2011**, *39*, 1823–1832; f) J. B. Bramsen, M. M. Pakula, T. B. Hansen, C. Bus, N. Langkjær, D. Odadzic, R. Smicius, S. L. Wengel, J. Chattopadhyaya, J. W. Engels, P. Herdewijn, J. Wengel, J. Kjems, *Nucleic Acids Res.* **2010**, *38*, 5761–5773; g) N. M. Snead, J. R. Escamilla-Powers, J. J. Rossi, A. P. McCaffrey, *Mol. Ther. Nucleic Acids* **2013**, *2*, e103.
- [12] a) A. Pasternak, F. J. Hernandez, L. M. Rasmussen, B. Vester, J. Wengel, *Nucleic Acids Res.* **2011**, *39*, 1155–1164; b) T. B. Jensen, J. R. Henriksen, B. E. Rasmussen, L. M. Rasmussen, T. L. Andresen, J. Wengel, A. Pasternak, *Bioorg. Med. Chem.* **2011**, *19*, 4739–4745.
- [13] K. K. Karlsen, T. B. Jensen, J. Wengel, *J. Org. Chem.* **2009**, *74*, 8838–8841.
- [14] V. L. Malinovskii, D. Wenger, R. Häner, *Chem. Soc. Rev.* **2010**, *39*, 410–422.
- [15] M. E. Østergaard, P. J. Hrdlicka, *Chem. Soc. Rev.* **2011**, *40*, 5771–5788.
- [16] a) U. B. Christensen, E. B. Pedersen, *Nucleic Acids Res.* **2002**, *30*, 4918–4925; b) U. B. Christensen, E. B. Pedersen, *Helv. Chim. Acta* **2003**, *86*, 2090–2097; c) A. Pasternak, E. Kierzek, K. Pasternak, A. Fraczkak, D. H. Turner, R. Kierzek, *Biochemistry* **2008**, *47*, 1249–1258.
- [17] a) V. V. Filichev, E. B. Pedersen, *J. Am. Chem. Soc.* **2005**, *127*, 14849–14858; b) V. V. Filichev, I. V. Astakhova, A. D. Malakhov, V. A. Korshun, E. B. Pedersen, *Nucleic Acids Symp. Ser.* **2008**, *52*, 347–348; c) V. V. Filichev, I. V. Astakhova, A. D. Malakhov, V. A. Korshun, E. B. Pedersen, *Chem. Eur. J.* **2008**, *14*, 9968–9980; d) U. V. Schneider, I. Geci, N. Johnk, N. D. Mikkelsen, E. B. Pedersen, G. Lisby, *PLoS One* **2011**, *6*, e20565.
- [18] K. K. Karlsen, A. Okholm, J. Kjems, J. Wengel, *Bioorg. Med. Chem.* **2013**, *21*, 6186–6190.
- [19] T. L. Netzel, M. Zhao, K. Nafisi, J. Headrick, M. S. Sigman, B. E. Eaton, *J. Am. Chem. Soc.* **1995**, *117*, 9119–9128.
- [20] a) N. Amann, E. Pandurski, T. Fiebig, H.-A. Wagenknecht, *Angew. Chem.* **2002**, *114*, 3084–3087; *Angew. Chem. Int. Ed.* **2002**, *41*, 2978–2980; b) N. Amann, H.-A. Wagenknecht, *Synlett* **2002**, 687–691; c) E. Mayer, L. Valis, R. Huber, N. Amann, H.-A. Wagenknecht, *Synthesis* **2003**, 2335–2340.
- [21] P. Kaden, E. Mayer-Enthart, A. Trifonov, T. Fiebig, H.-A. Wagenknecht, *Angew. Chem.* **2005**, *117*, 1662–1666; *Angew. Chem. Int. Ed.* **2005**, *44*, 1636–1639.
- [22] a) E. Mayer-Enthart, H.-A. Wagenknecht, *Angew. Chem.* **2006**, *118*, 3451–3453; *Angew. Chem. Int. Ed.* **2006**, *45*, 3372–3375; b) E. Mayer-Enthart, C. Wanger, J. Barbaric, H.-A. Wagenknecht, *Tetrahedron* **2007**, *63*, 3434–3439.
- [23] N. Amann, E. Pandurski, T. Fiebig, H.-A. Wagenknecht, *Chem. Eur. J.* **2002**, *8*, 4877–4883.
- [24] I. J. Lee, M. Park, T. Joo, B. H. Kim, *Mol. BioSyst.* **2012**, *8*, 486–490.
- [25] A. S. Wabha, A. Esmaeili, M. J. Damha, R. H. E. Hudson, *Nucleic Acids Res.* **2010**, *38*, 1048–1056.
- [26] Y.-C. Shih, T.-C. Chien, *Tetrahedron* **2011**, *67*, 3915–3923.
- [27] A. Rajendran, S. Nakano, N. Sugimoto, *Chem. Commun.* **2010**, *46*, 1299–1301.
- [28] a) I. J. Lee, J. W. Yi, B. H. Kim, *Chem. Commun.* **2009**, 5383–5385; b) I. J. Lee, B. H. Kim, *Chem. Commun.* **2012**, *48*, 2074–2076.
- [29] M. J. Cavaluzzi, P. N. Borer, *Nucleic Acids Res.* **2004**, *32*, e13.

Received: September 3, 2013

Published online on November 25, 2013